Performance Recovery of Phase Change Materials (PCMs)-Modified Limestone Calcined Clay Cement (LC^3) Composite Through Air-Void Control Using a Silicone-Based Defoamer

Yoon Tung Chan[1], Nor Hasanah Abdul Shukor Lim[2,*], Shafiq Ishak[2,*], Mostafa Samadi[3], Shek Poi Ngian[2], Hong Yee Kek[4], and Shea Qin Tan[1]

[1]*Faculty of Civil Engineering, University of Technology Malaysia (UTM), Johor Bahru, Johor 81310, Malaysia*

[2]*UTM Construction Research Center (CRC), Department of Structure and Materials, Faculty of Civil Engineering, University of Technology Malaysia (UTM), Johor Bahru, Johor 81310, Malaysia*

[3]*Institute of Energy Infrastructure, Universiti Tenaga Nasional, Jalan IKRAM-UNITEN, Kajang, 43000, Selangor, Malaysia*

[4]*School of the Built Environment, Universiti of Reading Malaysia, Johor, Malaysia*

Abstract: Limestone calcined clay cement (LC^3) has emerged as a promising low-carbon alternative to ordinary Portland cement (OPC) due to its reduced clinker content and associated carbon footprint. In parallel, integrating phase change materials (PCMs) into cementitious composites offers a pathway to enhance building thermal regulation through latent heat storage. However, hydrophobic PCMs may adversely affect fresh workability and hardened performance, particularly by promoting entrapped air and increasing porosity. This study investigates the incorporation of capric acid (CA) as an organic PCMs through partial cement replacement (0%, 1%, 5%, and 10% by mass) in OPC and LC^3 mortars. In this context, the mortar is a functional organic–inorganic composite, where the organic PCMs phase contributes thermal energy storage functionality. Unlike most PCMs studies focused on OPC systems, this work emphasises LC^3 and identifies air-void control as a critical mechanism for performance recovery in LC^3–PCMs composites. It also evaluates the effectiveness of a silicone-based defoamer (0.15% by mass of the total mixture) in mitigating air-related performance losses. Fresh flowability, hardened density, ultrasonic pulse velocity, and compressive strength were determined up to 28 days. Results showed that increasing CA content reduced flowability, density, UPV, and compressive strength in both OPC and LC^3 systems, indicating that hydrophobic PCMs inclusion adversely affected matrix continuity. However, the incorporation of a silicone-based defoamer enabled performance recovery in both OPC and LC^3 composites by improving matrix compactness through air-void control. Overall, the results demonstrate that air-void control is critical for PCMs-modified mortars, and that defoamer addition provides a practical approach to improve the performance of LC^3–PCMs systems while maintaining their sustainability benefits.

Keywords: Limestone calcined clay cement (LC^3), Phase change materials (PCMs), Defoamer, Capric acid.

1. INTRODUCTION

Ordinary Portland cement (OPC) remains the dominant binder for concrete and mortar production, yet its manufacture is associated with substantial greenhouse gas emissions due to both energy-intensive clinker production and process emissions from limestone calcination [1]. The cement sector is consistently identified as one of the major industrial contributors to global emissions [2], which has intensified pressure on the construction industry to adopt lower-carbon binders and to improve the environmental performance of cement-based materials.

In response, several alternative or reduced-clinker binder technologies have been developed and increasingly investigated, including alkali-activated materials (AAMs) and geopolymers [3, 4], as well as wider deployment of supplementary cementitious materials (SCMs) [5]. Among these approaches, limestone calcined clay cement (LC^3) has gained significant interest as a practical, scalable, and resource-efficient system because it is designed to reduce clinker content while maintaining mechanical performance suitable for structural applications [6].

LC^3 is a blended cement system typically composed of clinker, calcined clay, and limestone [7]. The synergy between calcined clay and limestone enables a higher clinker substitution level than conventional limestone or clay blending alone [8]. In many reported formulations, clinker factors as low as approximately 50% can be achieved with comparable strength development to OPC and improvements in selected durability indicators, depending on mixture design and curing conditions [9]. In parallel, the reduction in clinker content provides a direct pathway to lowering embodied carbon, with studies reporting that LC^3-type blends can deliver substantial CO_2 savings relative to OPC [8].

*Address correspondence to this author at the UTM Construction Research Center (CRC), Department of Structure and Materials, Faculty of Civil Engineering, University of Technology Malaysia (UTM), Johor Bahru, Johor 81310, Malaysia; E-mail: norhasanah@utm.my; shafiq.ishak@utm.my

Received on 09-01-2026 Accepted on 10-02-2026 Published on 12-02-2026

E-ISSN: 2311-8717/26

Alongside binder decarbonisation, improving the operational energy efficiency of buildings is another key strategy to reduce life-cycle environmental impacts [10]. Cementitious materials with thermal energy storage capability have therefore received increasing attention, particularly through the integration of phase change materials (PCMs) [11-13]. PCMs can absorb and release significant quantities of latent heat during phase transitions, which can dampen indoor temperature fluctuations and reduce cooling loads [14]. Such effects are attractive for building envelopes and interior components, especially in climates where daily temperature cycles align with the PCMs transition range.

PCMs used in cementitious composites are commonly categorised as organic (such as paraffins and fatty acids), inorganic (such as salt hydrates), and eutectic systems [15, 16]. Organic PCMs are widely studied because of their chemical stability and favourable cycling behaviour [17]. In this study, capric acid (CA) was selected as the PCMs due to its phase change temperature range that aligns well with typical indoor comfort temperatures and its relatively high latent heat capacity [18-20].

Despite these benefits, the incorporation of PCMs into cementitious systems commonly introduces drawbacks that limit broader adoption. Reductions in fresh workability and hardened mechanical performance have been frequently reported [17, 21]. These effects arise from PCMs dilution of the reactive binder fraction, weak mechanical contribution of the PCM phase, and increased heterogeneity in the hardened matrix [22]. A practical and often under-emphasised issue is the tendency for hydrophobic PCMs to promote foam stabilisation and entrapped air during mixing, which increases porosity and disrupts matrix continuity [11].

The use of defoaming agents provides a potential route to mitigate these air-entrainment and foam-stabilisation issues. Defoamers are designed to suppress and control foams in cementitious suspensions, reducing the persistence of air voids that can become weak points after hardening [23]. Evidence from cementitious mortar studies indicates that appropriate defoamer use can modify pore structure and improve mechanical performance by limiting entrapped air [24]. This strategy is therefore promising for enabling PCMs integration while preserving the sustainability advantages of LC^3.

Against this background, the present study examines the feasibility of incorporating CA as a PCMs through partial binder replacement in both OPC and LC^3 mortar systems, with specific emphasis on LC^3 as the primary low-carbon binder platform. While previous studies have investigated PCMs integration in OPC-based systems and the mechanical behaviour of LC^3 independently, limited attention has been given to the combined challenges of PCMs incorporation in LC^3, particularly the role of air-void formation in governing performance loss. This study uniquely highlights air-void control as a key mechanism influencing the fresh and hardened behaviour of LC^3–PCM mortars. CA was introduced at replacement levels of 0%, 1%, 5%, and 10% by mass, and a silicone-based defoamer was applied at a constant dosage to evaluate its effectiveness in mitigating air-related performance losses. By systematically evaluating the effectiveness of a silicone-based defoamer in mitigating entrapped air, this work provides new insight into how mechanical performance recovery can be achieved without compromising the sustainability advantages of LC^3.

2. MATERIALS AND METHODS

2.1. Materials

The OPC used in this study was obtained from the Structures and Materials Laboratory at Universiti Teknologi Malaysia (UTM) and was originally manufactured by YTL Cement, Malaysia. The calcined clay and limestone were supplied by Kaolin Sdn. Bhd., Malaysia. The oxide compositions of all raw materials were determined using X-ray fluorescence (XRF), with the results summarised in Table **1**. The true densities

Table 1: Oxide Compositions of Raw Materials

Oxides	OPC (wt.%)	Calcined Clay (wt.%)	Limestone (wt.%)
SiO2	15.12	65.22	0.21
Al2O3	4.08	25.42	0.62
CaO	72.05	0.13	94.27
Fe2O3	3.13	2.03	0.09
K2O	0.97	4.32	-
MgO	0.64	1.26	4.42
SO3	3.03	-	-
Others	0.98	1.62	0.39

of the materials were measured using a helium pycnometer (PentaPyc 5200e, Quantachrome, USA), and the corresponding values are presented in Figure **1**. The mineralogical characteristics of the raw materials were analysed using X-ray diffraction (XRD) with a SmartLab diffractometer (Rigaku, Japan), and the diffraction patterns are shown in Figure **2**. The OPC primarily consists of tricalcium silicate (C_3S) and dicalcium silicate (C_2S), accompanied by minor phases of tricalcium aluminate (C_3A) and tetracalcium aluminoferrite (C_4AF). For the calcined clay, residual kaolinite peaks were still detected despite the calcination process, together with dominant quartz and minor anatase phases. An amorphous hump observed between 15° and 35° 2θ indicates the presence of metakaolin, consistent with previous findings [25]. In contrast, the limestone exhibits a pronounced calcite crystalline phase with a minor contribution from dolomite. The particle size distribution of the raw materials was determined by laser diffraction (Mastersizer 3000, Malvern Panalytical, UK) as displayed in Figure **3**. Table **2** provides the distribution percentiles of the raw materials. The surface morphology of the raw materials was characterised using scanning electron microscopy (SEM) (JSM-IT300LV, JEOL, Japan) shown in Figure **4**.

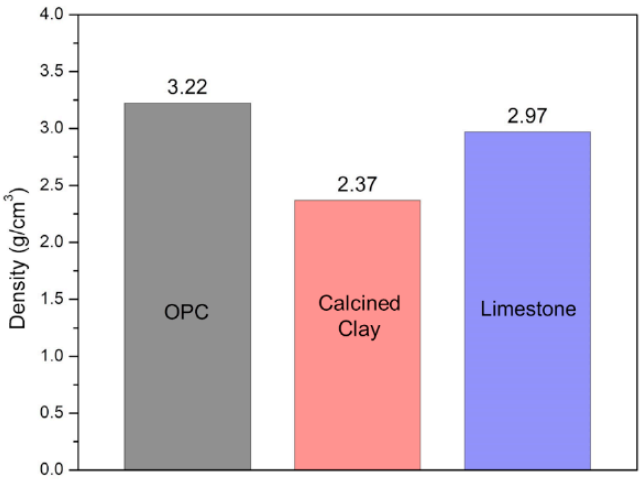

Figure 1: Density of raw materials.

The PCMs employed in this investigation was capric acid (CA), with a chemical formula of C10H20O2 and a molar mass of 172.27 g/mol. The material had a certified purity greater than 98% and was obtained from Macklin Biochemical Co., Ltd. (Shanghai, China), as illustrated in Figure **5a**. The differential scanning calorimetry (DSC) results of CA are presented in Figure **6**. The melting phase initiated at 31.75 °C and reached a peak at 33.80 °C, with an associated latent heat of 153.29 J g-1. Upon cooling, solidification commenced

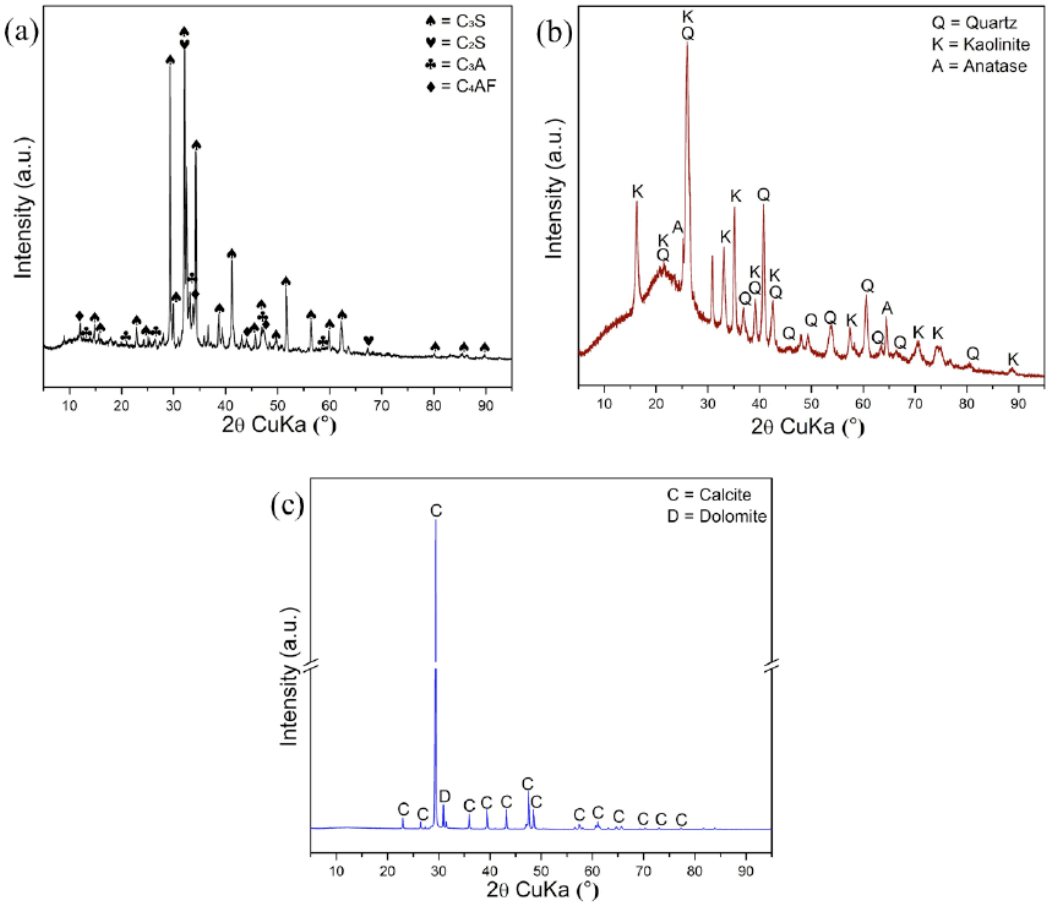

Figure 2: Diffraction patterns of (**a**) OPC, (**b**) calcined clay, and (**c**) limestone.

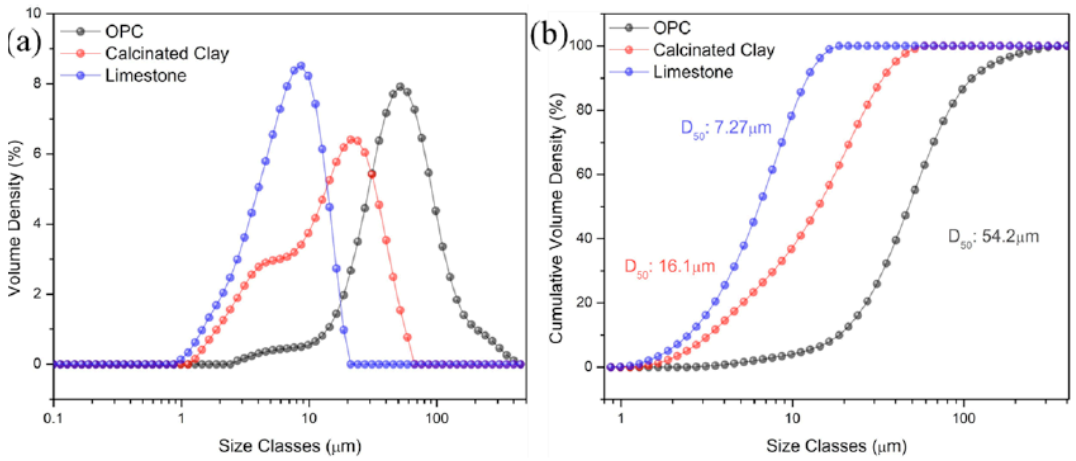

Figure 3: (**a**) Volume density and (**b**) cumulative particle size distributions of the raw materials.

Table 2: Size Distribution of Raw Materials

Raw Materials	OPC	Calcined Clay	Limestone
D90 (μm)	127	3.70	2.80
D50 (μm)	54.2	16.1	7.27
D10 (μm)	21.3	38.3	13.9

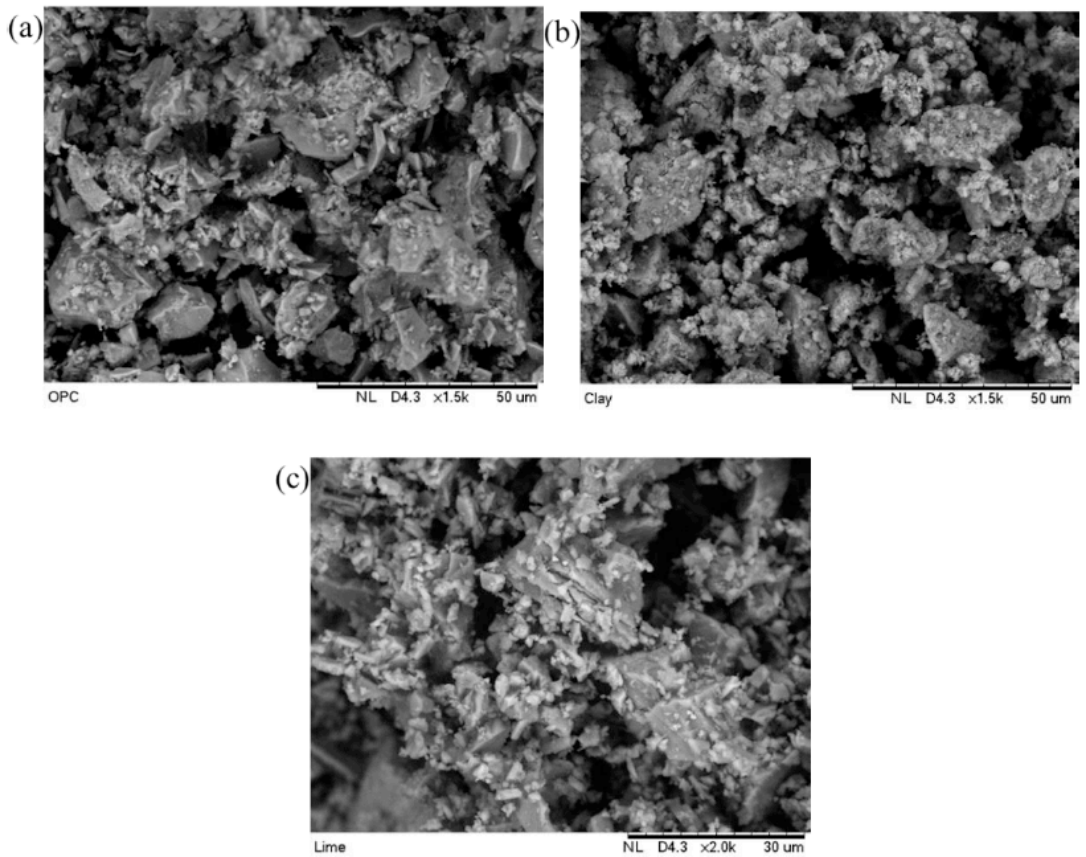

Figure 4: Surface morphology of (**a**) OPC, (**b**) calcined clay, and (**c**) limestone.

at 26.94 °C, with a peak crystallisation temperature of 26.57 °C and a latent heat of 159.14 J g-1. A silicone-based defoamer was also incorporated in the mixtures to control entrapped air. The defoamer was supplied as a viscous, milky-white liquid, sourced from Dchemie Malaysia, and is shown in Figure **5b**.

Figure 5: (**a**) Capric acid and (**b**) Silicone defoamer.

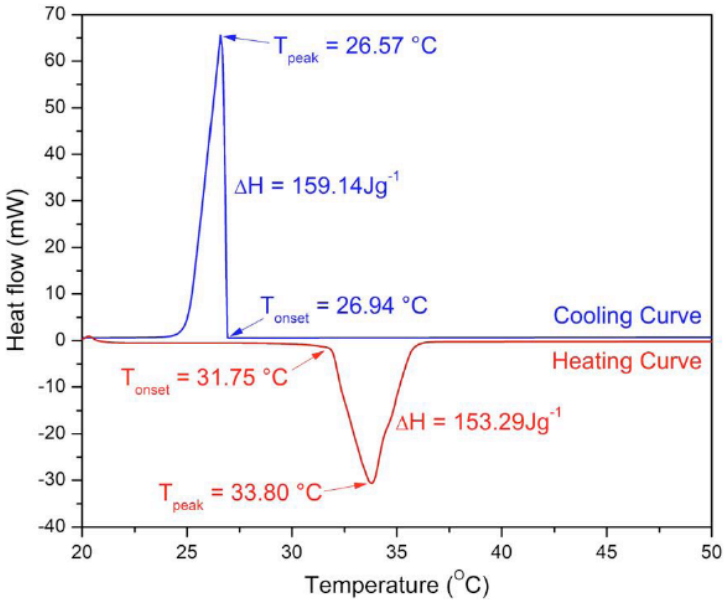

Figure 6: DSC Capric acid.

2.2. Mix Design

All mortar mixtures were prepared using a cement-to-sand ratio of 1:3 and a water-to-cement ratio of 0.60. CA was incorporated as a partial replacement of cement at dosage levels of 0%, 1%, 5%, and 10% by mass. The control mixture consisted of OPC as the sole cementitious material, with the corresponding mix proportions presented in Table **3**. For the LC^3 system, the binder composition comprised 55% OPC, 30% calcined clay, and 15% limestone. The mixture proportions of LC^3 mortars incorporating CA are summarised in Table **4** and were selected based on established LC^3 formulations reported in the literature [26]. A silicone-based defoamer was added to all OPC and LC^3 mixtures at a constant dosage of 0.15% by mass of the total mixture, with the detailed proportions provided in Tables **5** and **6**.

Table 3: Mixture Proportions of OPC-CA Samples

Samples	OPC (kg/m^3)	Water (kg/m^3)	Sand (kg/m^3)	CA (kg/m^3)
OPC_CA_0	506.00	253.04	1518.00	0.00
OPC_CA_1	500.96	253.04	1518.00	5.04
OPC_CA_5	480.72	253.04	1518.00	25.28
OPC_CA_10	455.44	253.04	1518.00	50.26

Table 4: Mixture Proportions of LC^3-CA Samples

Samples	OPC (kg/m^3)	Calcined clay (kg/m^3)	Limestone (kg/m^3)	Water (kg/m^3)	Sand (kg/m^3)	CA (kg/m^3)
LC^3_CA_0	278.3	151.8	75.9	253.04	1518.00	0.00
LC^3_CA_1	275.5	150.3	75.1	253.04	1518.00	5.04
LC^3_CA_5	264.4	144.2	72.1	253.04	1518.00	25.28
LC^3_CA_10	250.5	136.6	68.3	253.04	1518.00	50.26

Table 5: Mixture Proportions of OPC-CA-Defoamer Samples

Samples	OPC (kg/m^3)	Water (kg/m^3)	Sand (kg/m^3)	CA (kg/m^3)	Defoamer (kg/m^3)
OPC_CA_0	506.00	253.04	1518.00	0.00	3.42
OPC_CA_1	500.96	253.04	1518.00	5.04	3.42
OPC_CA_5	480.72	253.04	1518.00	25.28	3.42
OPC_CA_10	455.44	253.04	1518.00	50.26	3.42

Table 6: Mixture Proportions of LC^3-CA-Defoamer Samples

Samples	Density (kg/m^3)						
	OPC	Calcined clay	Limestone	Water	Sand	CA	Defoamer
LC^3_CA_0	278.3	151.8	75.9	253.04	1518.0	0.00	3.42
LC^3_CA_1	275.5	150.3	75.1	253.04	1518.0	5.04	3.42
LC^3_CA_5	264.4	144.2	72.1	253.04	1518.0	25.28	3.42
LC^3_CA_10	250.5	136.6	68.3	253.04	1518.0	50.26	3.42

2.3. Test Methods

Thermal performance tests were not included in this study, as the primary objective was to evaluate the influence of PCM incorporation and air-void control on the fresh and mechanical behaviour of LC^3-based composite mortars. The thermal characteristics of capric acid have been widely reported in the literature, and the focus of the present work is on enabling structural reliability of PCM-modified LC^3 systems.

2.3.1. Fresh Properties

The fresh-state behaviour of the mortar mixtures was characterised by flowability measurements conducted in accordance with ASTM C1437 [27]. "Standard Test Method for Flow of Hydraulic Cement Mortar". Fresh mortar was placed into a flow mould in two layers, each layer being lightly tamped to ensure uniform filling. The mould was then lifted vertically, and the flow table was dropped 25 times within 15 s. The resulting spread diameter of the mortar was measured along two perpendicular directions and averaged to determine the flow value.

2.3.2. Density

The density of the hardened mortar specimens was determined in accordance with ASTM C642 [28]. "Standard Test Method for Density, Absorption, and Voids in Hardened Concrete". The density was calculated based on the measured mass and specimen volume as prescribed by the standard.

2.3.3. Ultrasonic Pulse Velocity (UPV) Test

Ultrasonic pulse velocity (UPV) testing was conducted on the mortar specimens in compliance with ASTM C597 [29]. "Standard Test Method for Ultrasonic Pulse Velocity Through Concrete" for mortar samples". For each mixture, the reported UPV values represent the average of three specimens tested at curing ages of 1, 7, 14, and 28 days. For mixtures incorporating the defoamer, UPV measurements were carried out only at 28 days. Early-age UPV measurements were not performed for defoamer-modified mixtures because the primary purpose of defoamer incorporation was to evaluate its influence on the final hardened matrix compactness through air-void control rather than on early hydration kinetics.

2.3.4. Compressive Strength Test

Compressive strength tests were conducted in accordance with ASTM C109 [30] using a universal testing machine (Eco Smartz Automatic Compression Machine, 3000 kN). A constant loading rate of 0.9 kN/s

was applied during testing. The reported compressive strength values correspond to the average of three specimens evaluated at curing ages of 1, 7, 14, and 28 days.

3. RESULTS AND DISCUSSION

3.1. Fresh Properties

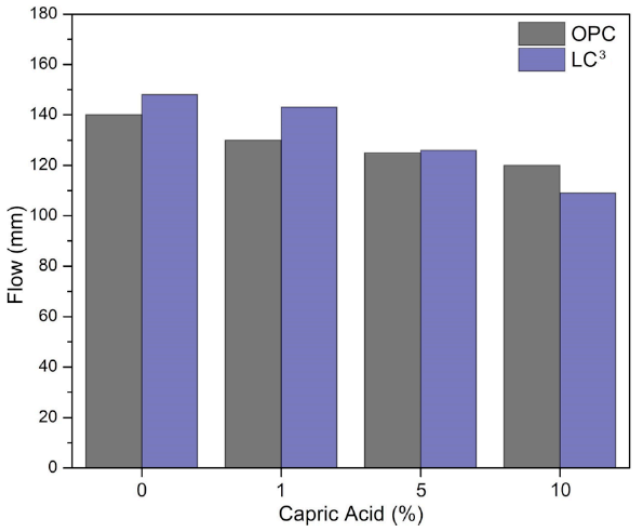

Figure 7: Flowability of OPC and LC^3 fresh mortar with CA replacement at different percentages.

Figure **7** illustrates the flowability of fresh OPC and LC^3 mortars incorporating different CA replacement levels. A consistent reduction in flow diameter is observed for both systems as the CA content increases. For the OPC mortar, the control mixture without CA exhibited a flow diameter of 140 mm, which progressively decreased to 130 mm, 125 mm, and 120 mm for CA replacement levels of 1%, 5%, and 10%, respectively. A similar trend was observed for the LC^3 mortars, where the flow diameter reduced from 148 mm at 0% CA to 143 mm, 126 mm, and 109 mm as the CA content increased. The magnitude of flow reduction observed in this study is consistent with previous reports on PCM-modified cementitious materials. Cunha *et al*. [31] and Drissi *et al*. [21] reported that PCM incorporation increases water demand and internal friction in mortar systems, particularly when hydrophobic PCMs are used.

The reduction in flowability with increasing CA dosage can be attributed to the hydrophobic nature of capric acid [32], which disrupts the uniform distribution of free water within the fresh mortar matrix and weakens the lubrication effect required for particle mobility. Owing to its limited affinity for water, CA tends to segregate within the mix and locally impede water–solid interactions, thereby increasing internal friction among cementitious and aggregate particles. As a result, the presence of CA promotes particle agglomeration and restricts mortar spread. Consistent trends have been reported in previous studies on PCMs-modified cementitious systems, confirming the reduction in flowability associated with increasing PCMs content [21, 31, 33]. The more pronounced reduction in flow observed in LC^3 mixtures at higher CA contents may be associated with the higher fineness and surface reactivity of calcined clay, which increases water demand and intensifies the sensitivity of LC^3 systems to the incorporation of hydrophobic PCMs.

3.2. Density of Mortars

Figure **8** presents the density of OPC and LC^3 mortars incorporating CA at different replacement levels and curing ages. In general, the density of both mortar systems increases with curing age, reflecting the progressive hydration and densification of the cementitious matrix. However, the inclusion of CA results in a noticeable reduction in hardened mortar density across all replacement levels. At 28 days, the OPC control mixture exhibited a density of approximately 2200 kg/m³, which decreased to 2080,

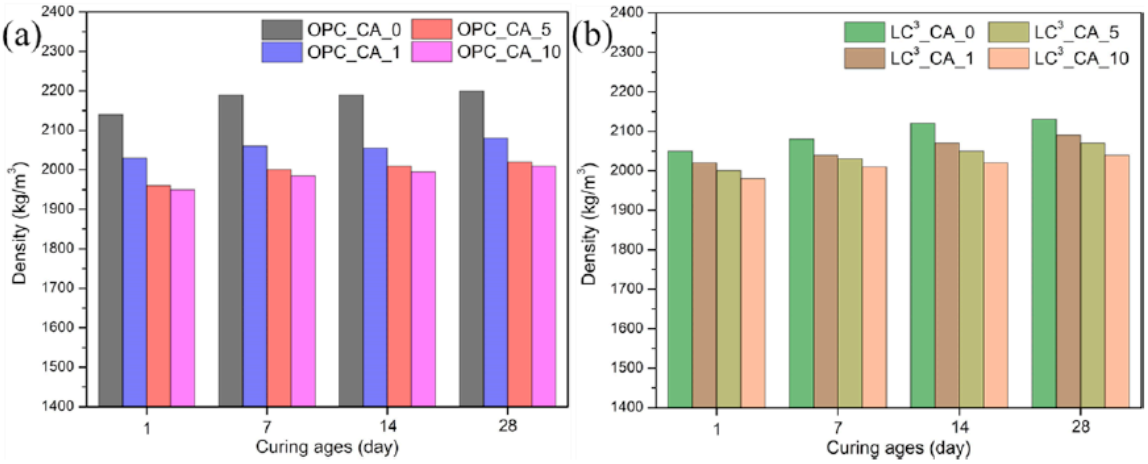

Figure 8: Density of (**a**) OPC and (**b**) LC^3 fresh mortar with CA replacement at different percentages.

2020, and 2010 kg/m³ with CA replacement levels of 1%, 5%, and 10%, respectively. A similar trend was observed for the LC^3 mortars, where the 28-day density of the control sample was 2130 kg/m³ and declined to 2090, 2070, and 2040 kg/m³ as the CA content increased.

The reduction in density associated with CA incorporation can be attributed to the lower intrinsic density of CA compared with cement, as well as its hydrophobic nature, which promotes air entrapment and disrupts particle packing within the hardened matrix [31, 33]. In addition, the presence of hydrophobic organic PCMs has been reported to locally interfere with water distribution during mixing and early hydration, which can hinder matrix densification and result in increased porosity and lower bulk density [34]. These observations highlight the importance of mitigating air entrapment effects when incorporating CA, thereby justifying the use of a defoaming agent in the present study.

3.3. Ultrasonic Pulse Velocity

The 28-day UPV results for OPC and LC^3 mortars incorporating CA are presented in Figure **9**. A clear reduction in UPV is observed with increasing CA content for both binder systems, indicating a progressive deterioration in internal matrix continuity. For OPC mortars, the control sample exhibited a UPV of 4.32 km/s, which decreased to 3.79, 3.41, and 3.24 km/s with 1%, 5%, and 10% CA incorporation, respectively. A similar trend was recorded for LC^3 mortars, where the control mixture showed a UPV of 3.89 km/s, declining to 3.68, 3.55, and 3.27 km/s as the CA dosage increased.

The reduction in UPV can be attributed primarily to the physical behaviour of CA within the cementitious system. As a hydrophobic organic compound, CA does not integrate into the hydration products and instead forms dispersed phases within the matrix [20]. These phases create regions of lower stiffness and density contrast relative to the surrounding hydrated cement, which disrupts the continuity of solid-phase wave transmission paths. In addition, CA incorporation is associated with increased entrapped air and localised heterogeneity, both of which increase acoustic impedance mismatches inside the material [35]. These discontinuities cause greater scattering and attenuation of ultrasonic waves, resulting in lower measured pulse velocities. The LC^3 mortars show lower baseline UPV values than OPC due to the different binder composition system of calcined clay, which increases water demand and makes the matrix more sensitive to the presence of dispersed hydrophobic phases [36]. Consequently, CA-induced heterogeneity has a stronger influence on the internal transmission behaviour of LC^3 mixtures.

3.4. Compressive Strength

The 28-day compressive strength results of OPC and LC^3 mortars incorporating CA are presented in Figure **10**. A systematic reduction in strength is observed with increasing CA replacement in both binder systems. This trend closely mirrors the reductions observed in density and UPV, indicating a strong relationship between matrix continuity, internal integrity, and load-bearing capacity. For OPC mortars, the control mixture achieved a 28-day compressive strength of 25.5 MPa. The incorporation of CA then resulted in strength reductions of approximately 24%, 41%, and 63% at replacement levels of 1%, 5%, and 10%, respectively. LC^3 mortars showed a control strength of 16.4 MPa, with corresponding reductions of approximately 18%, 32%, and 41% at the same CA contents. The magnitude of reduction increases with CA dosage, demonstrating the progressive influence of CA on the internal structure of the mortar.

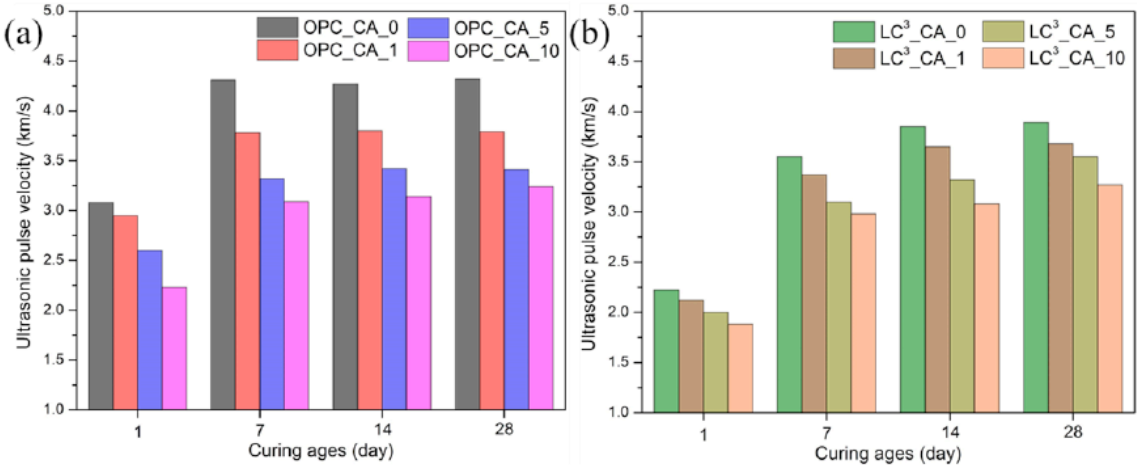

Figure 9: UPV of (**a**) OPC and (**b**) LC^3 fresh mortar with CA replacement at different percentages.

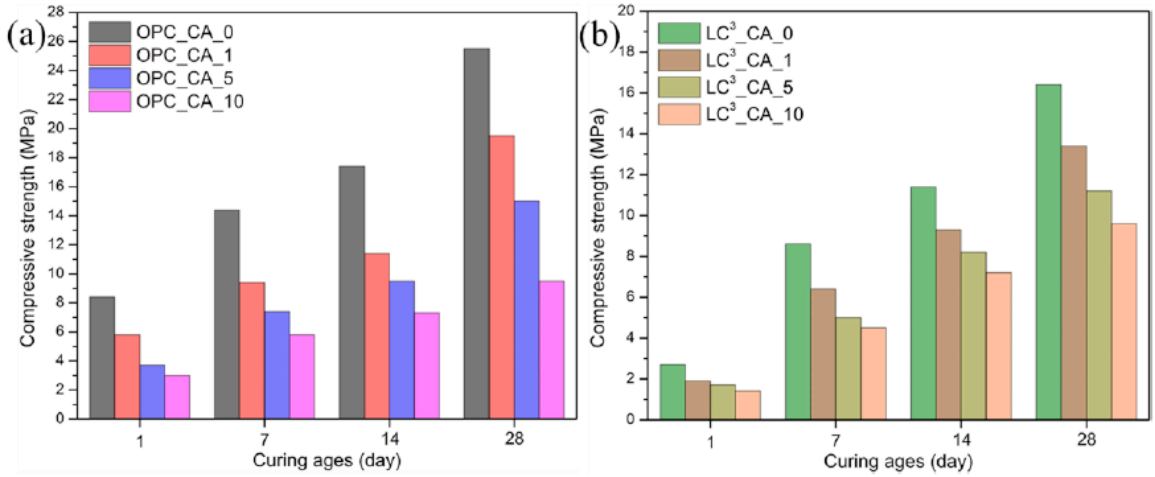

Figure 10: Compressive strength of (**a**) OPC and (**b**) LC^3 fresh mortar with CA replacement at different percentages.

The reduction in compressive strength can first be attributed to the dilution effect, as CA replaces a portion of the cementitious binder. Since CA is a non-cementitious material and does not participate in hydration reactions, its incorporation reduces the amount of reactive binder available to form strength-contributing hydration products, leading to a lower volume of load-bearing solid phases. Beyond dilution, CA exists within the matrix as dispersed low-stiffness organic domains that are mechanically weaker than the surrounding hydrated skeleton [20, 35]. These inclusions interrupt stress transfer pathways and reduce the effective cross-sectional area resisting compressive load. Similar strength reductions have been reported in previous studies incorporating capric acid or other organic PCMs into cementitious systems, where the non-structural nature of PCM phases and the associated increase in internal discontinuities led to comparable declines in compressive strength. Reported reductions in the literature commonly range between approximately 15% to 50%, depending on PCM type, dosage, and incorporation method [19, 21, 33], which aligns well with the magnitude of strength loss observed in the present study.

3.5. Effect of Defoamer Addition on Mortar Properties

3.5.1. Fresh Properties

Figure **11** illustrates the flowability of OPC and LC^3 mortars incorporating CA with and without the addition of a silicone-based defoamer. The inclusion of defoamer significantly improved the flow behaviour of CA-modified mixtures, confirming its effectiveness in mitigating the adverse fresh-state effects associated with hydrophobic PCM incorporation. For OPC mortars, defoamer addition increased the flow diameter by approximately 23-25% across all CA contents. LC^3 mortars also exhibited improved flowability, although to a lesser extent, with increases of approximately 3-7%.

The improvement in flowability is attributed to the ability of the silicone-based defoamer to destabilise and eliminate entrapped air bubbles generated during mixing [24]. In CA-modified mortars, the hydrophobic

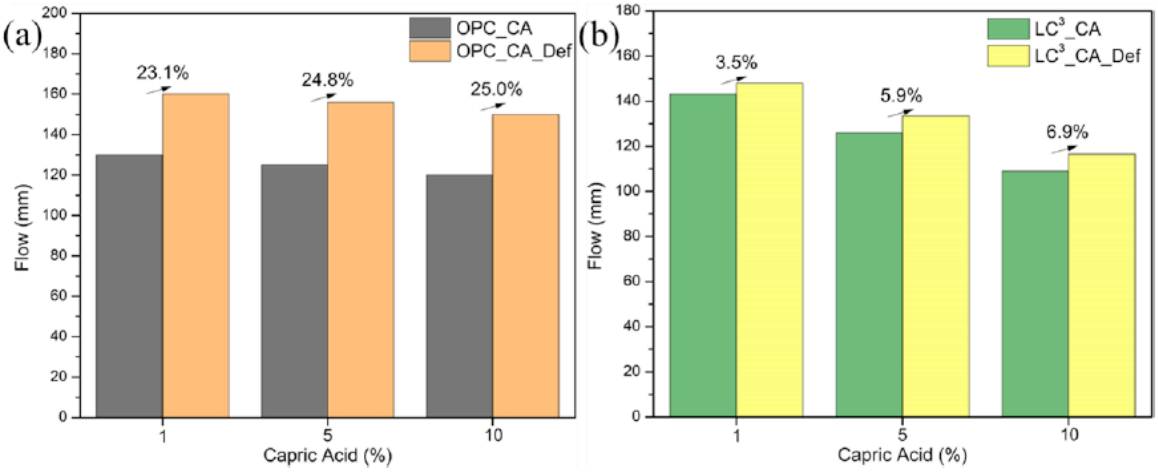

Figure 11: Flowability of (**a**) OPC and (**b**) LC^3 mortars incorporating different CA percentages with defoamer.

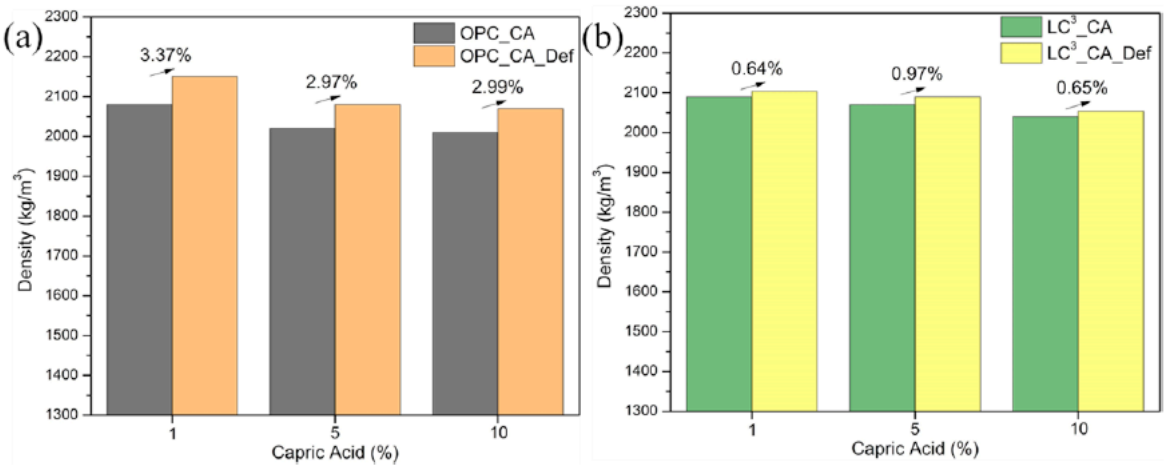

Figure 12: Hardened density of (**a**) OPC and (**b**) LC^3 mortars with varying CA replacement levels in the presence of defoamer at 28 days.

nature of CA promotes air entrapment and disrupts water distribution, increasing internal friction and restricting mortar spread. By reducing entrained air and improving particle packing, the defoamer enhances the effectiveness of the lubricating water phase. Overall, the results demonstrate that defoamer incorporation is essential for maintaining workable consistency in CA-modified mortars.

3.5.2. Hardened Properties

Figure **12** shows the 28-day density of OPC and LC^3 mortars incorporating CA in the presence of defoamer. Compared with the mixtures without defoamer (Figure **8**), all CA-modified mortars exhibit higher densities. For OPC mortars, density increased by approximately 3% across all CA replacement levels. LC^3 mortars showed smaller but consistent improvements of about 0.6–1.0%.

The increase in density confirms that the silicone-based defoamer effectively reduced entrapped air within the matrix. In CA-modified mortars, the hydrophobic nature of capric acid promotes air bubble stabilisation during mixing, leading to increased porosity and reduced packing efficiency [37]. The defoamer destabilises air–liquid interfaces and facilitates bubble escape, resulting in improved particle packing and a more compact hardened structure [23]. The smaller density improvement observed in LC^3 mortars may be related to their finer binder system, which already contributes to relatively dense packing, thereby reducing the relative influence of air removal.

The 28-day UPV results in Figure **13** show a consistent increase in pulse velocity for all mixtures incorporating defoamer. For OPC mortars, UPV improved by approximately 3–12%, while LC^3 mortars showed increases of about 3–4% compared with mixtures without defoamer. The UPV improvement corresponds well with the density results, confirming enhanced internal continuity of the matrix. Since ultrasonic wave propagation is highly sensitive to voids and internal discontinuities, the reduction in entrapped air leads to more continuous transmission paths. Consequently, the UPV reduction observed previously in CA-modified mortars (Figure **9**) arises from both

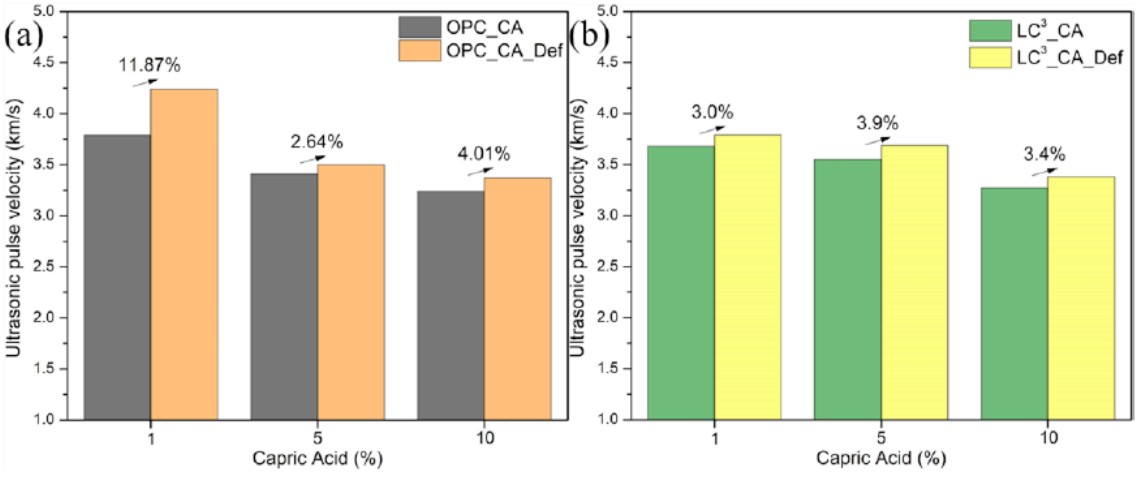

Figure 13: UPV of (**a**) OPC and (**b**) LC^3 mortars with varying CA replacement levels in the presence of defoamer at 28 days.

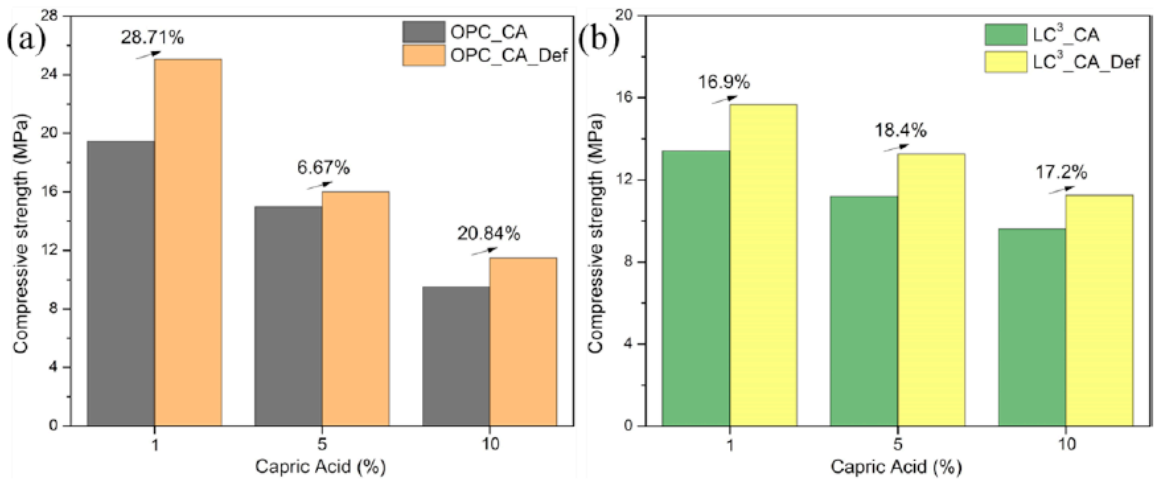

Figure 14: Compressive strength of (**a**) OPC and (**b**) LC^3 mortars with varying CA replacement levels in the presence of defoamer at 28 days.

PCMs inclusion and air entrapment, with the latter being partially reversible through defoamer addition.

Figure **14** presents the 28-day compressive strength of OPC and LC^3 mortars incorporating CA in the presence of defoamer. The inclusion of defoamer leads to a clear strength enhancement for all mixtures compared with those without air control. For OPC mortars, compressive strength increased by approximately 7–29%, depending on CA content. LC^3 mortars also showed consistent improvements, with strength increases of about 17–18% across the CA replacement levels. The magnitude of recovery in LC^3 mixtures is particularly notable given their lower baseline strength compared with OPC.

The strength improvement aligns closely with the trends observed in density and UPV (Figure **12** and **13**), confirming that the defoamer enhances internal compactness and matrix continuity by reducing entrapped air. Since compressive strength is highly sensitive to void content and internal discontinuities, the reduction of air-induced porosity increases the effective load-bearing cross-sectional area and improves stress transfer within the hydrated matrix [38]. Although LC^3 mortars exhibit lower absolute strength than OPC due to their reduced clinker content and different hydration chemistry [9], the present results demonstrate that part of the strength loss associated with PCMs incorporation originates from secondary air entrapment rather than solely the non-cementitious nature of CA. The defoamer effectively mitigates this secondary mechanism, allowing LC^3–PCMs mortars to achieve significantly improved structural performance while retaining the environmental advantages of the LC^3 system.

From a practical perspective, the highest CA replacement level (10%) resulted in substantial strength reductions, even with defoamer incorporation, which may limit its suitability for structural applications. The inclusion of high PCMs contents primarily serves to illustrate the sensitivity of LC^3-based composite systems to PCM-induced heterogeneity and air-void formation. Based on the present results, lower replacement levels in the range of 1–5% provide a more balanced compromise between mechanical performance and potential thermal functionality. At these levels, strength recovery through air-void control remains effective while avoiding excessive deterioration of structural properties. Therefore, moderate PCMs dosages are recommended for practical implementation of LC^3–PCM composite mortars in building applications.

4. CONCLUSION

This study evaluated the incorporation of CA as a PCMs in OPC and LC^3 mortars and evaluated the effectiveness of a silicone-based defoamer in mitigating the adverse effects associated with PCMs inclusion. The results showed that CA reduced the flowability of both OPC and LC^3 mortars due to its hydrophobic nature, which disrupted water distribution and increased internal friction among particles. This effect was more pronounced in LC^3 systems because of the higher fineness and water demand of calcined clay. The inclusion of CA also resulted in reductions in hardened density, UPV, and compressive strength in both binder systems. These changes were attributed to the lower intrinsic density and non-cementitious nature of CA, together with increased internal heterogeneity and air entrapment.

The addition of a silicone-based defoamer effectively improved both fresh and hardened properties of CA-modified mortars. Density increased by approximately 3% in OPC and up to 1% in LC^3

mixtures, while UPV improved by about 3–12%. Compressive strength recovery reached up to 29% in OPC mortars and approximately 17–18% in LC^3 mortars. These improvements indicate that a considerable portion of the performance loss in PCMs-modified mortars originates from air entrapment rather than solely from PCMs substitution.

Although LC^3 mortars exhibited lower absolute strength compared with OPC due to reduced clinker content and different hydration chemistry, the use of defoamer significantly mitigated the mechanical drawbacks associated with PCMs incorporation. This finding is particularly important from a sustainability perspective, as LC^3 is designed to reduce clinker consumption and associated carbon emissions. The combination of LC^3 and CA therefore offers a pathway for developing multifunctional cementitious materials that integrate thermal energy storage while maintaining improved mechanical reliability through effective air-void control. For practical applications, moderate PCM replacement levels (approximately 1–5%) are recommended to balance mechanical performance with thermal energy storage potential. Overall, the study highlights that air-void management is a critical factor in PCMs-integrated cementitious systems. While thermal performance was not experimentally evaluated in this study, the selected PCM possesses well-established latent heat storage properties, and the findings herein address the structural feasibility necessary for future thermally functional LC^3 composites. Further research is recommended to investigate the long-term mechanical stability and thermal cycling performance of LC^3–PCM mortars in building envelope applications, together with direct microstructural and pore structure characterisation (*e.g.*, SEM and porosity analysis) to verify the air-void control mechanism proposed in this study.

ACKNOWLEDGMENT

This research was supported by Universiti Teknologi Malaysia (UTM) under the Geran Penyelidik Baharu (Q.J130000.2709.03K90) and UTM Fundamental Research Grant (Q.J130000.3822.24H26).

CONFLICTS OF INTEREST

The author declared no conflicts of interest.

REFERENCES

[1] S. Sbahieh, G. McKay, A. Nurdiawati, S.G. Al-Ghamdi, The sustainability of partial and total replacement of Ordinary Portland Cement: A deep dive into different concrete mixtures through life cycle assessment, Journal of Building Engineering 108 (2025) 112830. https://doi.org/10.1016/j.jobe.2025.112830

[2] F. Belaïd, How does concrete and cement industry transformation contribute to mitigating climate change challenges?, Resources, Conservation & Recycling Advances 15 (2022) 200084. https://doi.org/10.1016/j.rcradv.2022.200084

[3] Y.T. Chan, N.H.A.S. Lim, S. Ishak, M. Samadi, S.P. Ngian, H.Y. Kek, S.Q. Tan, Mechanical and Microstructural Performances of One-Part Alkali-Activated Fly Ash Mortars with Thermally Activated Palm Oil Decanter Cake, Journal of Composites and Biodegradable Polymers 13 (2025) 183-201. https://doi.org/10.12974/2311-8717.2025.13.16

[4] Y.T. Chan, N.H. Abdul Shukor Lim, S.A. Abd Latif, S. Ishak, P.S. Lee, S.Q. Tan, A. Azhar, J.J. Moy, H.Y. Kek, Scientometric Review of One-Part Geopolymer Composites, International Conference on Intelligent Information Technologies, Springer, 2018, pp. 407-416. https://doi.org/10.1007/978-981-96-3804-8_36

[5] B. Lothenbach, K. Scrivener, R.D. Hooton, Supplementary cementitious materials, Cement and Concrete Research 41(12) (2011) 1244-1256. https://doi.org/10.1016/j.cemconres.2010.12.001

[6] Y.-S. Wang, S. Oh, S. Ishak, X.-Y. Wang, S. Lim, Recycled glass powder for enhanced sustainability of limestone calcined clay cement (LC^3) mixtures: mechanical properties, hydration, and microstructural analysis, Journal of Materials Research and Technology 27 (2023) 4012-4022. https://doi.org/10.1016/j.jmrt.2023.10.245

[7] K. Hosen, B. Chen, Limestone calcined clay cement (LC^3): A review of materials, properties, production and environmental impact, Journal of Building Engineering 112 (2025) 113672. https://doi.org/10.1016/j.jobe.2025.113672

[8] K. Scrivener, F. Martirena, S. Bishnoi, S. Maity, Calcined clay limestone cements (LC^3), Cement and Concrete Research 114 (2018) 49-56. https://doi.org/10.1016/j.cemconres.2017.08.017

[9] J. Sun, F. Zunino, K. Scrivener, Hydration and phase assemblage of limestone calcined clay cements (LC^3) with clinker content below 50 %, Cement and Concrete Research 177 (2024) 107417. https://doi.org/10.1016/j.cemconres.2023.107417

[10] F.S. Hafez, B. Sa'di, M. Safa-Gamal, Y.H. Taufiq-Yap, M. Alrifaey, M. Seyedmahmoudian, A. Stojcevski, B. Horan, S. Mekhilef, Energy Efficiency in Sustainable Buildings: A Systematic Review with Taxonomy, Challenges, Motivations, Methodological Aspects, Recommendations, and Pathways for Future Research, Energy Strategy Reviews 45 (2023) 101013. https://doi.org/10.1016/j.esr.2022.101013

[11] S. Ishak, M. Yio, J. Moon, S. Mandal, S. Sasui, N.H. Abdul Shukor Lim, X.-Y. Wang, Y.-S. Wang, M.M. Al Bakri Abdullah, P.N. Shek, Hydration and microstructural development of cement pastes incorporating diatomaceous earth, expanded perlite, and shape-stabilized phase change materials (SSPCMs), Construction and Building Materials 468 (2025) 140483. https://doi.org/10.1016/j.conbuildmat.2025.140483

[12] S. Ishak, S. Mandal, H.-S. Lee, D.-E. Lee, Z. Chen, Structure-property correlation of thermally activated nano-size phase change material in the cementitious system, Journal of Building Engineering 66 (2023) 105871. https://doi.org/10.1016/j.jobe.2023.105871

[13] S. Mandal, A.C. Mendhe, Y.N. Singhbabu, H.-S. Lee, T. Park, S. Ishak, Physical, chemical, and thermal properties of porous expanded perlite-based phase change composite and their effects on the hydration kinetics, Case Studies in Construction Materials 22 (2025) e04510. https://doi.org/10.1016/j.cscm.2025.e04510

[14] S. Ishak, H. Lgaz, S. Mandal, R.J. Adnin, D.-E. Lee, H.-S. Lee, N.S. Mohammad Harmay, M.M. Al Bakri Abdullah, X.-Y. Wang, H.-M. Yang, Multi-technique investigation on the surface interaction of diatomaceous earth with organic phase change material: Experimental and molecular dynamics aspects, Journal of Molecular Liquids 391 (2023) 123292. https://doi.org/10.1016/j.molliq.2023.123292

[15] Ł. Mika, E. Radomska, K. Sztekler, A. Gołdasz, W. Zima, Review of Selected PCMs and Their Applications in the Industry and Energy Sector, Energies, 2025, p. 1233. https://doi.org/10.3390/en18051233

[16] A. Anand, M. Mansor, K. Sharma, A. Shukla, A. Sharma, M.I.H. Siddiqui, K.K. Sadasivuni, N. Priyadarshi, B. Twala, A comprehensive review on eutectic phase change materials: Development, thermophysical properties, thermal stability, reliability, and applications, Alexandria Engineering Journal 112 (2025) 254-280. https://doi.org/10.1016/j.aej.2024.10.054

[17] R. Baetens, B.P. Jelle, A. Gustavsen, Phase change materials for building applications: A state-of-the-art review, Energy and Buildings 42(9) (2010) 1361-1368. https://doi.org/10.1016/j.enbuild.2010.03.026

[18] S. Ishak, S. Mandal, H. Lgaz, D.G. Atinafu, N.S. Mohammad Harmay, H.-S. Lee, N. Abdul Shukor Lim, M.M.A.B. Abdullah, H.-M. Yang, Microscopic molecular insights of different carbon chain fatty acids on shape-stabilized phase change composite, Journal of Thermal Analysis and Calorimetry 149(17) (2024) 9203-9221. https://doi.org/10.1007/s10973-024-13539-0

[19] G. Hekimoğlu, M. Nas, M. Ouikhalfan, A. Sarı, V.V. Tyagi, R.K. Sharma, Ş. Kurbetci, T.A. Saleh, Silica fume/capric acid-stearic acid PCM included-cementitious composite for thermal controlling of buildings: Thermal energy storage and mechanical properties, Energy 219 (2021) 119588. https://doi.org/10.1016/j.energy.2020.119588

[20] F. Meng, L. Dong, Y. Wu, X. Shu, Y. Guo, Q. Ran, Effects and mechanisms of capric acid/silica capsule on water absorption reduction of cement paste, Construction and Building Materials 404 (2023) 133208. https://doi.org/10.1016/j.conbuildmat.2023.133208

[21] S. Drissi, T.-C. Ling, K.H. Mo, A. Eddhahak, A review of microencapsulated and composite phase change materials: Alteration of strength and thermal properties of cement-based materials, Renewable and Sustainable Energy Reviews 110 (2019) 467-484. https://doi.org/10.1016/j.rser.2019.04.072

[22] M.M. Alsaadawi, M. Amin, A.M. Tahwia, Thermal, mechanical and microstructural properties of sustainable concrete incorporating Phase change materials, Construction and Building Materials 356 (2022) 129300. https://doi.org/10.1016/j.conbuildmat.2022.129300

[23] M. Qiao, J. Wu, N. Gao, G. Shan, F. Shen, J. Chen, B. Zhu, Preparation and Properties of Different Polyether-Type Defoamers for Concrete, Materials, 2022, p. 7492. https://doi.org/10.3390/ma15217492

[24] J. Hu, Y. Xie, Z. Liu, Z. Weng, Y. Wang, K. Li, Effectiveness of air entraining agent and defoamer on the bubble distribution of fresh mortar under different mixing methods, IOP Conference Series: Earth and Environmental Science 371(4) (2019) 042012. https://doi.org/10.1088/1755-1315/371/4/042012

[25] L. Yuan, Y. Ma, J. Zhang, J. Men, T. Sun, H. Zhao, H. Wu, H. Wang, S. Dai, Orthogonal analysis and mechanism of compressive strength and microstructure of the metakaolin-fly ash geopolymer, Case Studies in Construction Materials 17 (2022) e01154. https://doi.org/10.1016/j.cscm.2022.e01154

[26] F. Zunino, K. Scrivener, The reaction between metakaolin and limestone and its effect in porosity refinement and mechanical properties, Cement and Concrete Research 140 (2021) 106307. https://doi.org/10.1016/j.cemconres.2020.106307

[27] ASTM C1437, Standard Test Method for Flow of Hydraulic Cement Mortar, ASTM International, West Conshohocken, 2020, p. 2.

[28] ASTM C642, Standard Test Method for Density, Absorption, and Voids in Hardened Concrete, ASTM International, West Conshohocken, 2021, p. 3.

[29] ASTM C597, Standard Test Method for Ultrasonic Pulse Velocity Through Concrete, ASTM International, West Conshohocken, 2022, p. 4.

[30] ASTM C109, Standard Test Method for Compressive Strength of Hydraulic Cement Mortars (Using 2-in. or [50-mm] Cube Specimens), ASTM International, West Conshohocken, 2022, p. 11.

[31] S. Cunha, M. Lima, J.B. Aguiar, Influence of adding phase change materials on the physical and mechanical properties of cement mortars, Construction and Building Materials 127 (2016) 1-10. https://doi.org/10.1016/j.conbuildmat.2016.09.119

[32] J.L. Trenzado, C. Benito, M. Atilhan, S. Aparicio, Hydrophobic Deep eutectic Solvents based on cineole and organic acids, Journal of Molecular Liquids 377 (2023) 121322. https://doi.org/10.1016/j.molliq.2023.121322

[33] A. Figueiredo, J. Lapa, R. Vicente, C. Cardoso, Mechanical and thermal characterization of concrete with incorporation of microencapsulated PCM for applications in thermally activated slabs, Construction and Building Materials 112 (2016) 639-647. https://doi.org/10.1016/j.conbuildmat.2016.02.225

[34] M. Łach, K. Pławecka, A. Bąk, M. Adamczyk, P. Bazan, B. Kozub, K. Korniejenko, W.-T. Lin, Review of Solutions for the Use of Phase Change Materials in Geopolymers, Materials, 2021, p. 6044. https://doi.org/10.3390/ma14206044

[35] K. Yu, M. Jia, W. Tian, Y. Yang, Y. Liu, Enhanced thermo-mechanical properties of cementitious composites via red mud-based microencapsulated phase change material: Towards energy conservation in building, Energy 290 (2024) 130301. https://doi.org/10.1016/j.energy.2024.130301

[36] L. Ferrari, V. Bortolotti, N. Mikanovic, M. Ben-Haha, E. Franzoni, Influence of calcined clay on workability of mortars with low-carbon cement, Nanoworld Journal 9(Special Issue 2) (2023) S30-S34. https://doi.org/10.17756/nwj.2023-s2-006

[37] H. Zhang, S. Mu, J. Cai, R. Chen, The impact of carboxylic acid type hydrophobic agent on compressive strength of cementitious materials, Construction and Building Materials 291 (2021) 123315. https://doi.org/10.1016/j.conbuildmat.2021.123315

[38] R. Abousnina, F. Aljuaydi, B. Benabed, M.H. Almabrok, V. Vimonsatit, A State-of-the-Art Review on the Influence of Porosity on the Compressive Strength of Porous Concrete for Infrastructure Applications, Buildings 15(13) (2025) 2311. https://doi.org/10.3390/buildings15132311

https://doi.org/10.12974/2311-8717.2026.14.01

© 2026 Chan *et al.*
This is an open-access article licensed under the terms of the Creative Commons Attribution License (http://creativecommons.org/licenses/by/4.0/), which permits unrestricted use, distribution, and reproduction in any medium, provided the work is properly cited.